genase structures, evolved independently. Remarkably, hydrogenases are the only metalloenzymes that use toxic CO and cyanide (or pyridinol) as metal ligands. Thus, hydrogenases are an impressive example of convergent evolutionary development as a consequence of specific biological and/or chemical restraints. However, the intrinsic physicochemical properties of the unique iron ligation pattern are not yet understood, nor are their implications for the technologically important H_2 activation reaction.

Despite the related low-spin iron centers, the enzymatic mechanism of [Fe]-hydrogenase differs fundamentally from that of the other types because of the different nature of the redox-active partner and the accompanying electron delivery mode. In [NiFe]- and [FeFe]-hydrogenases, the electrons of H_2 reduction flow one by one through the redox-active metals and several iron-sulfur clusters over a large distance to an electron acceptor. The active-site structures essentially remain fixed during H_2 cleavage, and H_2 reaches the deeply buried active site by a long diffusion channel. In [Fe]-hydrogenase, however, the found ternary reaction mechanism and the exchange between H_2 and protons of water solely in the presence of methenyl-H_4MPT$^+$ (*32*) (see partial structure in Fig. 2) suggests that methenyl-H_4MPT$^+$ directly accepts the hydride from H_2. This conclusion is supported by the x-ray structure, as the cleft between the peripheral and central units can accommodate the bulky methenyl-H_4MPT$^+$ molecule and the C14a atom can be positioned sufficiently close to the iron without causing severe clashes with the polypeptide chain (fig. S3). Because the intersubunit cleft in the holoenzyme is, in fact, too large for an optimal methenyl-H_4MPT$^+$ adjustment, we assume that its binding is accompanied by an induced-fit movement constituting the catalysis-competent active-site before each turnover. The expected large-scale conformational changes are reflected in the different positions of the peripheral unit relative to the central unit found in the structures of the holo- and apoenzymes (Fig. 3), mainly induced by crystal forces. H_2 can readily reach the solvent-exposed Fe center, which is probably encapsulated upon methenyl-H_4MPT$^+$ binding.

The most attractive hypothesis for the mechanism of H_2 cleavage in [Fe]-hydrogenases is based on a concerted action of the strong hydride acceptor methenyl-H_4MPT$^+$ and the Lewis acid Fe(II) that lowers the pK_a value of H_2, preferably when bound in a side-on conformation. The polarized H_2 ligated to the postulated binding site (Fig. 5) is attacked from the adjacent carbocation C14a of methenyl-H_4MPT$^+$ from the *Re*-face of the ring system (see Fig. 2), generating methylene-H_4MPT. Acceptors for the released proton within 6.5 Å from the iron include the Cys^{176} thiolate ligand, the pyridinol nitrogen, oxygen, and carboxyl oxygen as well as two conserved histidines, His^{14} and His^{201} (for the position of the two histidines relative to the iron, see fig. S1B). A His^{14} → Ala mutation drastically reduces the hydrogenase activity of the enzyme, whereas His^{201} → Ala has only a minor effect (table S2).

Although there are still many questions to be answered, the crystal structure allows us to draw the following conclusions: (i) The active-site iron is definitely mononuclear, not dinuclear as in the [FeFe]- and [NiFe]-hydrogenases. (ii) The presented structural data, together with results of studies using various spectroscopic methods [nuclear magnetic resonance (NMR), mass, IR, Mössbauer, and extended x-ray absorption fine structure (EXAFS) (*23*–*26*)] and information from mutational analysis (*25*), converge to a coherent result. (iii) The structures of the [Fe]-, [FeFe]-, and [NiFe]-hydrogenases are completely different but share features in their active site that can only have evolved convergently (Fig. 1). (iv) The detailed three-dimensional structure will allow density functional theory (DFT) calculations of energy profiles, which will help to exclude some of the proposed mechanisms of H_2 activation. (v) Model complexes can be constructed on the basis of the iron center of [Fe]-hydrogenase, and their analysis will provide further insight into its essential but not yet understood function in H_2 activation (*3*–*7*).

References and Notes

1. D. M. Heinekey, W. J. Oldham, *Chem. Rev.* **93**, 913 (1993).
2. G. J. Kubas, *Catal. Lett.* **104**, 79 (2005).
3. C. Tard *et al.*, *Nature* **433**, 610 (2005).
4. T. Liu, M. Y. Darensbourg, *J. Am. Chem. Soc.* **129**, 7008 (2007).
5. A. K. Justice *et al.*, *Inorg. Chem.* **46**, 1655 (2007).
6. S. Ogo *et al.*, *Science* **316**, 585 (2007).
7. X. Hu, B. S. Brunschwig, J. C. Peters, *J. Am. Chem. Soc.* **129**, 8988 (2007).
8. P. M. Vignais, B. Billoud, J. Meyer, *FEMS Microbiol. Rev.* **25**, 455 (2001).
9. A. Volbeda *et al.*, *Nature* **373**, 580 (1995).
10. E. Garcin *et al.*, *Structure* **7**, 557 (1999).
11. H. Ogata *et al.*, *J. Am. Chem. Soc.* **124**, 11628 (2002).
12. A. Volbeda *et al.*, *J. Biol. Inorg. Chem.* **10**, 239 (2005).
13. J. W. Peters, W. N. Lanzilotta, B. J. Lemon, L. C. Seefeldt, *Science* **282**, 1853 (1998).
14. Y. Nicolet, C. Piras, P. Legrand, C. E. Hatchikian, J. C. Fontecilla-Camps, *Structure* **7**, 13 (1999).
15. B. J. Lemon, J. W. Peters, *Biochemistry* **38**, 12969 (1999).
16. Y. Nicolet *et al.*, *J. Am. Chem. Soc.* **123**, 1596 (2001).
17. Z. Chen *et al.*, *Biochemistry* **41**, 2036 (2002).
18. M. Frey, *ChemBioChem* **3**, 153 (2002).
19. A. Silakov, E. J. Reijerse, S. P. J. Albracht, E. C. Hatchikian, W. Lubitz, *J. Am. Chem. Soc.* **129**, 11447 (2007).
20. S. Shima, R. K. Thauer, *Chem. Rec.* **7**, 37 (2007).
21. G. Buurman, S. Shima, R. K. Thauer, *FEBS Lett.* **485**, 200 (2000).
22. E. J. Lyon *et al.*, *Eur. J. Biochem.* **271**, 195 (2004).
23. S. Shima *et al.*, *Angew. Chem. Int. Ed.* **43**, 2547 (2004).
24. E. J. Lyon *et al.*, *J. Am. Chem. Soc.* **126**, 14239 (2004).
25. M. Korbas *et al.*, *J. Biol. Chem.* **281**, 30804 (2006).
26. S. Shima, E. J. Lyon, R. K. Thauer, B. Mienert, B. Bill, *J. Am. Chem. Soc.* **127**, 10430 (2005).
27. O. Pilak *et al.*, *J. Mol. Biol.* **358**, 798 (2006).
28. See supporting material on *Science* Online.
29. J. M. Rawson, R. E. P. Winpenny, *Coord. Chem. Rev.* **139**, 313 (1995).
30. S. Wolfe, N. Weinberg, Y. Hsieh, *Theor. Chem. Acc.* **118**, 265 (2007).
31. A. Böck, P. W. King, M. Blokesch, M. C. Posewitz, *Adv. Microb. Physiol.* **51**, 1 (2006).
32. S. Vogt, E. J. Lyon, S. Shima, R. K. Thauer, *J. Biol. Inorg. Chem.* **13**, 97 (2008).
33. Supported by the Max Planck Society, the Fonds der Chemischen Industrie, and the Bundesministerium für Bildung und Forschung (BioH$_2$ project). We thank H. Michel for continuous support, and the staff of beamline PXII at the Swiss Light Source for help during data collection. Coordinates of [Fe]-hydrogenase and [Fe]-hydrogenase complexed with cyanide have been deposited in the Research Collaboratory for Structural Bioinformatics Protein Data Bank under accession codes 3DAG and 3DAF.

Supporting Online Material

www.sciencemag.org/cgi/content/full/321/5888/572/DC1
Materials and Methods
Figs. S1 to S3
Tables S1 to S3
References

10 April 2008; accepted 5 June 2008
10.1126/science.1158978

Manipulating the Metazoan Mitochondrial Genome with Targeted Restriction Enzymes

Hong Xu, Steven Z. DeLuca, Patrick H. O'Farrell*

High copy number and random segregation confound genetic analysis of the mitochondrial genome. We developed an efficient selection for heritable mitochondrial genome (mtDNA) mutations in *Drosophila*, thereby enhancing a metazoan model for study of mitochondrial genetics and mutations causing human mitochondrial disease. Targeting a restriction enzyme to mitochondria in the germline compromised fertility, but escaper progeny carried homoplasmic mtDNA mutations lacking the cleavage site. Among mutations eliminating a site in the cytochrome c oxidase gene, *mt:CoI*^{A302T} was healthy, *mt:CoI*^{R301L} was male sterile but otherwise healthy, and *mt:CoI*^{R301S} exhibited a wide range of defects, including growth retardation, neurodegeneration, muscular atrophy, male sterility, and reduced life span. Thus, germline expression of mitochondrial restriction enzymes creates a powerful selection and has allowed direct isolation of mitochondrial mutants in a metazoan.

A typical animal cell contains hundreds to thousands of copies of the mitochondrial genome (mtDNA), which encodes 13 essential subunits of the electron transport chain complexes and RNAs (2 rRNAs and 22 tRNAs) required for mitochondrial translation (*1*, *2*). It is not clear how the genetic integrity of this amitotically distributed genome is main-

tained. Due to a high mutation rate, lack of recombination, and the presence of coresident genomes to protect mutant genomes from selection, mtDNA mutations should readily accumulate in cells (*3*). Indeed, a dramatic accumulation of mitochondrial mutations in somatic tissues appears to contribute to age-related disorders in humans (*4*), and numerous mutations on human mtDNA have been linked to maternally inherited diseases (*1*, *2*). The mitochondrial genome has not been very amenable to functional genetic studies in metazoans (*5*, *6*). Successful generation of trans-mitochondrial mice by hybridizing mtDNA-depleted embryonic stem cells and enucleated donor cells containing mtDNA mutations (*6*) has been constrained by the limited collections of donor cells carrying mtDNA mutations.

Targeting restriction enzymes to mitochondria can selectively compromise propagation of mtDNA that has a site targeted by the enzyme (*7*). We reasoned that expression of a restriction enzyme targeting wild-type mtDNA would create a selection allowing rare mutations lacking the restriction site to take over (fig. S1). XhoI has a single recognition site in the cytochrome c oxidase subunit I locus (*mt:CoI*) in the *Drosophila melanogaster* mitochondrial genome (fig. S2). It overlaps codons specifying three amino acid residues in a conserved region of CoI (Fig. 1E and fig. S3). *pMT-mitoXhoI*, which encodes XhoI fused to a mitochondrial targeting leader at its N terminus and a Myc tag at its C terminus (fig. S4), was used to establish S2 cell lines. MitoXhoI protein was specifically localized to mitochondria (fig. S4). Upon induction, the majority of the mtDNA was cleaved at the XhoI site (Fig. 1, A and B), demonstrating that MitoXhoI can efficiently target the wild-type mitochondrial genome.

To test the consequence of MitoXhoI expression in animals, we generated transgenic flies expressing *mitoXhoI* under the UASp promoter. Ubiquitous expression of *UAS-mitoXhoI* activated by a *tub-GAL4* driver blocked hatching of 95% of the embryos, and the remaining 5% died as first instar larvae. Selective expression of *UAS-mitoXhoI* in the eye primordium using an *eyeless-GAL4* driver ablated or greatly reduced the eye (Fig. 1C).

To select for heritable mitochondrial mutants, we used *nanos-GAL4* to activate *UAS-mitoXhoI* expression in germline cells, reasoning that those cells carrying XhoI-resistant mtDNA would survive to produce progeny carrying the mutant mtDNA (fig. S5). Most of the *UAS-mitoXhoI*/+; *nanos-Gal4*/+ flies were sterile, but about 1% of the females gave a few escaper progeny. Escapers all carried XhoI-resistant mtDNA (Fig. 1D), and no wild-type genomes were detected, which suggests that each mutant was homoplasmic. Sequencing identified single base pair mutations that eliminated the XhoI site (Fig. 1E). Three different sequence variants were recovered, *mt:CoI*^{A302T}, *mt:CoI*^{R301L}, and *mt:CoI*^{R301S}, all resulting in a single amino acid change (Fig. 1E). No secondary mutations were seen in these mutants, and each mutant was maternally inherited and conferred complete resistance to MitoXhoI in the eye (Fig. 1C).

We investigated whether any of these *mt:CoI* mutations were pathogenic. Only *mt:CoI*^{A302T} behaved as wild-type flies in the phenotypic analyses we conducted (table S1). *mt:CoI*^{R301L} flies were healthy, except that the males were sterile (table S1). Spermatogenesis appeared normal, and sperm were motile but reduced in number (movies S1 and S2). Sperm were transferred to the female during mating but were not stored in the sperm storage organs. Despite being sterile, male *mt:CoI*^{R301L} flies had similar cytochrome c oxidase activity and slightly higher adenosine triphosphate (ATP) levels than wild-type flies (fig. S6). It is not clear how a mitochondrial mutation selectively compromises sperm function, but, because transmission of mtDNA occurs through the female, it has been argued that such mutations can be sustained in a population (*8*) and could make a substantial contribution to male sterility (*9*). The *mt:CoI*^{R301S} allele exhibited markedly more severe phenotypes. The mutant had an extended larval phase (about 10 days at 25°C), and the mechanosensory bristles on the thorax were missing or thinned and shortened (Fig. 2, A and B). The males were sterile without any mature sperm, which suggests a defect in spermatogenesis. Female flies were fertile but produced only 20% as many progeny as did wild-type flies. The *mt-CoI*^{R301S} flies had about half the normal cytochrome c oxidase activity and significantly reduced ATP levels (fig. S6).

Because most mtDNA diseases in humans show neuropathy and myopathy, we examined the morphology of retina and indirect flight muscles to determine whether *mt:CoI*^{R301S} flies had similar defects. Young *mt:CoI*^{R301S} flies had the full complement of ommatidia components, although some rhabdomeres had slight morphogenetic defects (Fig. 2, C and D). However, the ommatidia of aged *mt:CoI*^{R301S}, but not wild-type flies, were disorganized and the rhabdomeres were shrunken or completely lost (Fig. 2E), indicating age-dependent degeneration of photoreceptor neurons.

Transmission electron microscopy (TEM) of flight muscle in wild-type and young *mt:CoI*^{R301S} flies revealed orderly muscle fibers and fused mitochondria with long and tubular cristae (Fig. 2, F and G). However, two weeks after adult eclosion, the *mt:CoI*^{R301S} mitochondria were small and fragmented, contained many vesicular structures, and

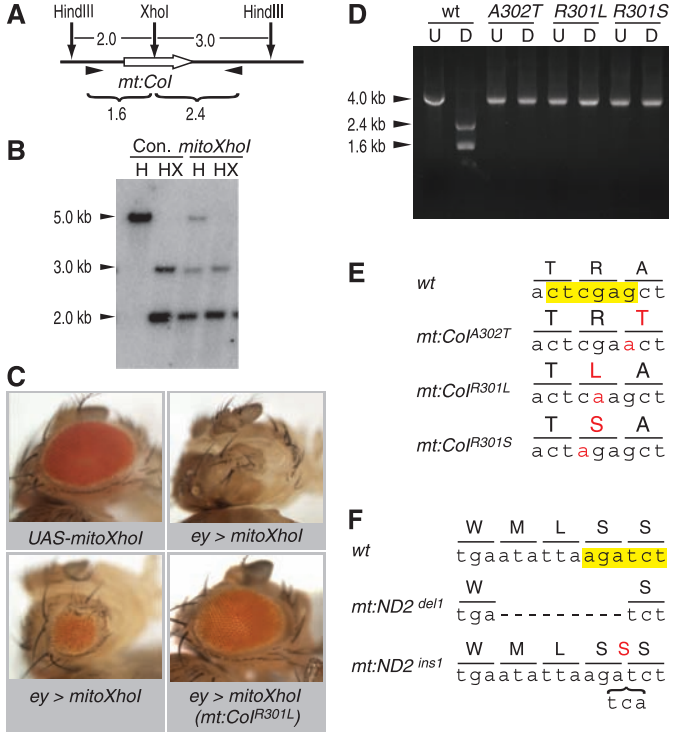

Fig. 1. Manipulation of mtDNA with a mitochondrially targeted XhoI (MitoXhoI). (**A**) Restriction map of a mitochondrial genomic region spanning cytochrome c oxidase subunit 1 (*mt:CoI*, thick white arrow). The size of each fragment is given in kb. (**B**) Total DNA was extracted from control (Con.) and *mitoXhoI*-expressing (*mitoXhoI*) S2 cells, digested with HindIII (H) or HindIII and XhoI (HX), and hybridized with probe against the *mt:CoI* gene. (**C**) *UAS-mitoXhoI*, when expressed under the control of *eyeless-Gal4* (*ey>mitoXhoI*), caused eye ablation or small eye, which was suppressed in flies containing XhoI-resistant mtDNA [*ey>mitoXhoI(mt:CoI*^{R301L})]. (**D**) mtDNAs were amplified using the pair of primers denoted as arrowheads in (A). U, undigested polymerase chain reaction (PCR) product; D, PCR product digested with XhoI. There are no detectable wild-type bands in any of the mutants. (**E**) Recovered mutant mtDNAs with mutations in the XhoI site (yellow). Mutated nucleotides and changed amino acid residues are highlighted in red. (**F**) Recovered mutant mitochondrial genomes with mutations affecting the BglII site (yellow). Dashed line represents a 9-nucleotide deletion. Bracket represents a 3-nucleotide insertion encoding an extra serine residue (red).

Department of Biochemistry and Biophysics, University of California at San Francisco, San Francisco, CA 94158–2200, USA.

*To whom correspondence should be addressed. E-mail: ofarrell@cgl.ucsf.edu

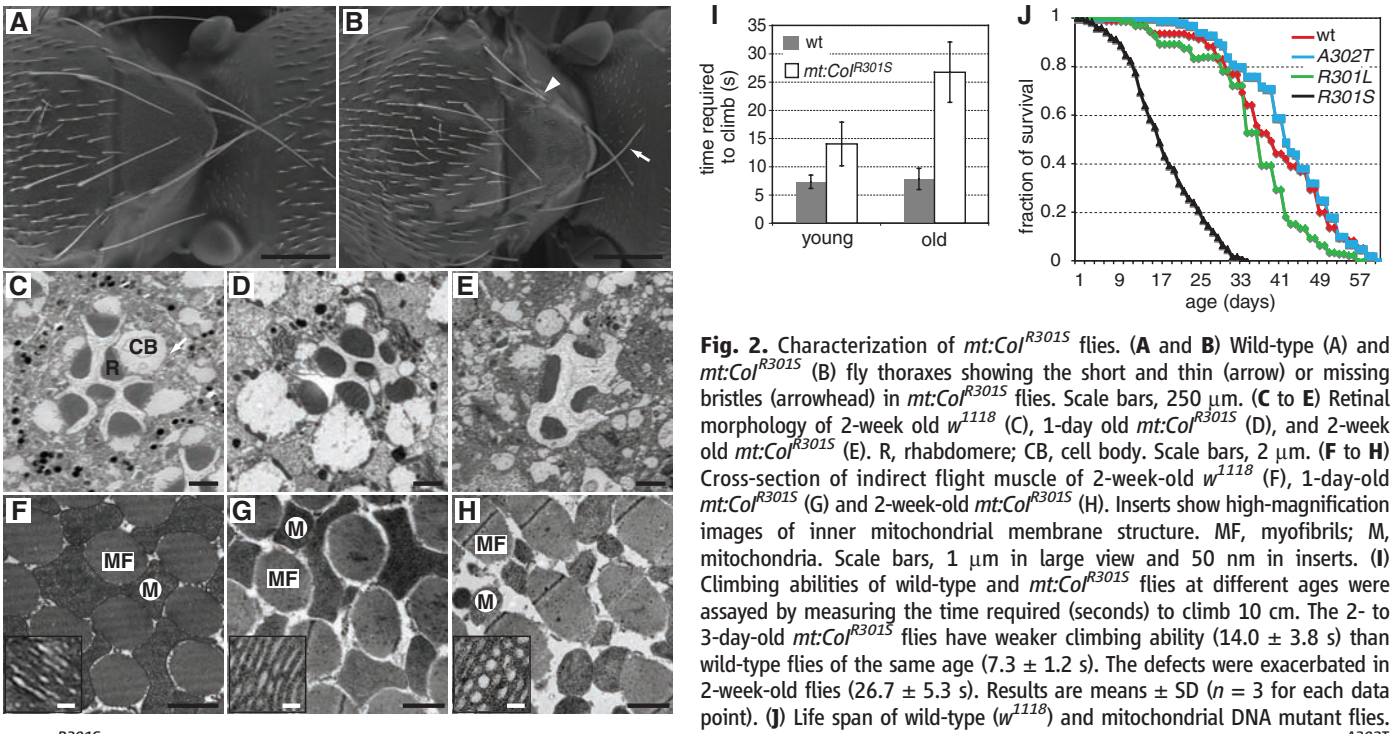

Fig. 2. Characterization of *mt:CoI*^{R301S} flies. (**A** and **B**) Wild-type (A) and *mt:CoI*^{R301S} (B) fly thoraxes showing the short and thin (arrow) or missing bristles (arrowhead) in *mt:CoI*^{R301S} flies. Scale bars, 250 μm. (**C** to **E**) Retinal morphology of 2-week old w^{1118} (C), 1-day old *mt:CoI*^{R301S} (D), and 2-week old *mt:CoI*^{R301S} (E). R, rhabdomere; CB, cell body. Scale bars, 2 μm. (**F** to **H**) Cross-section of indirect flight muscle of 2-week-old w^{1118} (F), 1-day-old *mt:CoI*^{R301S} (G) and 2-week-old *mt:CoI*^{R301S} (H). Inserts show high-magnification images of inner mitochondrial membrane structure. MF, myofibrils; M, mitochondria. Scale bars, 1 μm in large view and 50 nm in inserts. (**I**) Climbing abilities of wild-type and *mt:CoI*^{R301S} flies at different ages were assayed by measuring the time required (seconds) to climb 10 cm. The 2- to 3-day-old *mt:CoI*^{R301S} flies have weaker climbing ability (14.0 ± 3.8 s) than wild-type flies of the same age (7.3 ± 1.2 s). The defects were exacerbated in 2-week-old flies (26.7 ± 5.3 s). Results are means ± SD (n = 3 for each data point). (**J**) Life span of wild-type (w^{1118}) and mitochondrial DNA mutant flies. *mt:CoI*^{R301S} flies showed greatly reduced longevity, with a median life span of 17 days. The median life span of wild-type flies is 41 days. Neither *mt:CoI*^{A302T} nor *mt:CoI*^{R301L} flies displayed any significant alterations in life span compared with wild-type flies.

did not completely fill the intermyofibril space (Fig. 2H). Similar mitochondrial morphological defects were also reported in flies with a mutation in the mitochondrial *ATP6* locus (*10*). Moreover, when tested in a climbing assay, *mt:CoI*^{R301S} flies showed mobility defects enhanced by age, consistent with age-dependent neurodegeneration and myopathy (Fig. 2I). Beyond these age-dependent neurological and muscular dysfunctions, *mt:CoI*^{R301S} flies had substantially reduced longevity (Fig. 2J).

The pathologies associated with human mitochondrial DNA diseases often develop with age (*1*), much like the degenerative changes that we find for the *mt:CoI*^{R301S} allele. Because the mutations responsible for human mitochondrial disease usually affect only a fraction of the mitochondrial genomes (heteroplasmy), the progressive increase in the severity of the phenotype might be attributed to an increase in the load of mutant genomes in the affected tissues or to an inherent feature of the mitochondrial defect. Because the mutations we have selected are homoplasmic, the age-dependent degenerative phenotype must be inherent to the mutation.

There are 31 single-cutting restriction enzymes sites in *Drosophila* mtDNA, distributed within eight protein-encoding genes, two rRNAs and three tRNAs (table S2). To test the generality of our approach, we produced a *UASp*-regulated *mitoBglII* transgene that targets a single BglII site in the *mt:ND2* locus. After germline expression, we recovered two lines carrying mutations in *mt:ND2*. In contrast to the single base changes recovered in *mt:CoI*, one *mt:ND2* mutation is an in-frame deletion and the other is a three-nucleotide insertion (Fig. 1F). Use of the full panel of available enzymes will target the majority of the protein coding genes in *Drosophila* mtDNA and allow generation of multiple alleles, although we expect that alleles that completely eliminate respiratory activity will not be recovered as a result of lethality.

In the described selection for resistance to germline expression of mitochondrial restriction enzymes, roughly one out of several thousand germline precursor cells (PGCs) survived to produce progeny. Mice have about 50 PGCs, and this population is greatly expanded before definitive germ cell differentiation (*11*). Furthermore, one could employ the previously developed "mtDNA mutator mouse" carrying an error-prone mitochondrial DNA polymerase (*12*) to increase the frequency of enzyme-resistant mitochondrial genomes. If the frequency of mtDNA mutations in mice is similar to that in flies, generation of novel homoplasmic mitochondrial mutant mice by the described approach should be practical.

References and Notes

1. D. C. Wallace, *Annu. Rev. Genet.* **39**, 359 (2005).
2. R. W. Taylor, D. M. Turnbull, *Nat. Rev. Genet.* **6**, 389 (2005).
3. C. T. Bergstrom, J. Pritchard, *Genetics* **149**, 2135 (1998).
4. R. W. Taylor *et al.*, *J. Clin. Invest.* **112**, 1351 (2003).
5. M. P. Bayona-Bafaluy, P. Fernández-Silva, J. A. Enríquez, *Mitochondrion* **2**, 3 (2002).
6. S. M. Khan, R. M. Smigrodzki, R. H. Swerdlow, *Am. J. Physiol. Cell Physiol.* **292**, C658 (2007).
7. S. Srivastava, C. T. Moraes, *Hum. Mol. Genet.* **10**, 3093 (2001).
8. S. A. Frank, L. D. Hurst, *Nature* **383**, 224 (1996).
9. J. Spiropoulos, D. M. Turnbull, P. F. Chinnery, *Mol. Hum. Reprod.* **8**, 719 (2002).
10. A. M. Celotto *et al.*, *J. Neurosci.* **26**, 810 (2006).
11. P. P. Tam, M. H. Snow, *J. Embryol. Exp. Morphol.* **64**, 133 (1981).
12. A. Trifunovic *et al.*, *Nature* **429**, 417 (2004).
13. We thank members of O'Farrell laboratory for comments on the manuscripts; M.-L. Wong and M. Sepanski for technical help with TEM; M. Fuller and A. W. Shermoen for help with examination of spermatogenesis and sperm in female reproductive organs; and Bloomington Stock Center for providing some *Drosophila* stocks. This work is supported by an NIH RO1 grant and a Sandler Family Supporting Foundation award to P.H.O. H.X. is supported by a postdoctoral fellowship from the Larry L. Hillblom Foundation.

Supporting Online Material

www.sciencemag.org/cgi/content/full/321/5888/575/DC1
Materials and Methods
Figs. S1 to S6
Tables S1 and S2
References
Movies S1 and S2

8 May 2008; accepted 19 June 2008
10.1126/science.1160226

ERRATUM

Post date 5 December 2008

Reports: "Manipulating the metazoan mitochondrial genome with targeted restriction enzymes" by H. Xu *et al*. (25 July, p. 575). The caa codon in the *mt:CoI*^{R301L} mutant in Fig. 1E should encode a glutamine (Q) rather than the indicated leucine (L).

Manipulating the Metazoan Mitochondrial Genome with Targeted Restriction Enzymes

Hong Xu, Steven Z. DeLuca and Patrick H. O'Farrell

Science **321** (5888), 575-577.
DOI: 10.1126/science.1160226